

An acoustofluidic platform for non-contact trapping of cell-laden hydrogel droplets compatible with optical microscopy

Cite as: Biomicrofluidics 13, 044101 (2019); doi: 10.1063/1.5108583

Submitted: 30 April 2019 · Accepted: 20 June 2019 ·

Published Online: 11 July 2019



View Online



Export Citation



CrossMark

Anna Fornell,¹ Carl Johannesson,² Sean S. Searle,^{1,3} Axel Happstadius,² Johan Nilsson,² and Maria Tenje^{1,a)}

AFFILIATIONS

¹ Department of Engineering Sciences, Science for Life Laboratory, Uppsala University, Box 534, 751 21 Uppsala, Sweden

² Department of Biomedical Engineering, Lund University, Box 118, 221 00 Lund, Sweden

³ Department of Biomedical Engineering, Faculty of Engineering, National University of Singapore, 4 Engineering Drive 3 Block 4, #04-08, 117583 Singapore, Singapore

^{a)}maria.tenje@angstrom.uu.se

ABSTRACT

Production of cell-laden hydrogel droplets as miniaturized niches for 3D cell culture provides a new route for cell-based assays. Such production can be enabled by droplet microfluidics and here we present a droplet trapping system based on bulk acoustic waves for handling hydrogel droplets in a continuous flow format. The droplet trapping system consists of a glass capillary equipped with a small piezoelectric transducer. By applying ultrasound (4 MHz), a localized acoustic standing wave field is generated in the capillary, trapping the droplets in a well-defined cluster above the transducer area. The results show that the droplet cluster can be retained at flow rates of up to 76 $\mu\text{l}/\text{min}$, corresponding to an average flow speed of 3.2 mm/s. The system allows for important operations such as continuous perfusion and/or addition of chemical reagents to the encapsulated cells with *in situ* optical access. This feature is demonstrated by performing on-chip staining of the cell nuclei. The key advantages of this trapping method are that it is label-free and gentle and thus well-suited for biological applications. Moreover, the droplets can easily be released on-demand, which facilitates downstream analysis. It is envisioned that the presented droplet trapping system will be a valuable tool for a wide range of multistep assays as well as long-term monitoring of cells encapsulated in gel-based droplets.

Published under license by AIP Publishing. <https://doi.org/10.1063/1.5108583>

INTRODUCTION

During the last decade, the emergence of droplet microfluidics has opened up new possibilities in the biological sciences.^{1–5} In droplet microfluidics, droplets with a volume in the nl-pl range are created at high throughput. Typically, water-in-oil droplets containing bioparticles are generated, whereby each droplet serves as an isolated compartment for biological experiments and measurements. The small volumes dramatically decrease the chemical reagents and the biological sample needed for each analysis and lead to a reduction in both cost and environmental footprint. The applications of this technology include high throughput screening of cells,^{6,7} artificial cell generation,⁸ and tissue engineering.⁹

For applications involving cell culturing in droplets, the use of water-in-oil droplets holds certain limitations. Firstly, the microenvironment in water droplets differs considerably from the composition

of the human tissue. In the body, cells are surrounded by the extracellular matrix (ECM), which provides mechanical support and biochemical cues that are important for the cells.¹⁰ Secondly, water-in-oil droplets do not allow for easy exchange of nutrients and waste products in and out of the droplets, thus limiting long-term cell studies. In order to meet these limitations, hydrogel droplets can be used.^{11–13}

Hydrogels are a class of materials consisting of polymer chains arranged in a 3D network that can retain a large amount of water.¹⁴ Both droplets made of synthetically derived hydrogels such as polyethylene glycol¹⁵ and natural derived hydrogels such as alginate,¹⁶ hyaluronic acid,¹⁷ and gelatin methacryloyl¹⁸ have been demonstrated previously using microfluidic platforms.

The principle for generating hydrogel droplets is similar for generating water-in-oil droplets.^{11–13} In a microfluidic channel junction, the dispersed phase (in this case, the hydrogel precursor

solution and cells) meets an immiscible carrier fluid (typically an oil), resulting in the generation of monodisperse hydrogel droplets containing cells. The number of cells in each droplet is determined by the cell concentration in the precursor solution and follows the Poisson distribution.¹⁹ Depending on the hydrogel material, the droplets can be cross-linked using, for example, UV-light, a temperature change, or the addition of chemical agents.²⁰ Next, the cross-linked hydrogel droplets are washed several times and transferred from the oil phase to cell medium for further cultures.

Conventionally, the cross-linking and culture are performed off-chip in bulk, but it would be very advantageous to be able to handle droplets on-chip. Methods to trap droplets on-chip allow for crucial operations such as continuous perfusion, staining, and visual inspection of the droplets' contents. Previously presented technical solutions to trap droplets on-chip^{21–24} often rely either completely or to a large extent on physical obstacles to trap the droplets. This approach limits the diffusion of molecules into the droplets and complicates droplet release for downstream analysis.

In this work, we present a technical platform for noncontact trapping of hydrogel droplets using bulk acoustic waves and show that the method is well-suited for biological assays such as on-chip staining. As a model system, we use hyaluronic acid acrylamide (HA-Am) hydrogel droplets containing chondrocytes (SW1353). This combination of cell line and hydrogel material is chosen because hyaluronic acid is one of the main components of cartilage,^{25,26} making the model biologically relevant.

ACOUSTIC THEORY

Previously, acoustics have been used to trap and pattern particles such as cells, plastic microbeads, and vesicles in Microsystems,^{27–31} but this is the first time cell-laden hydrogel droplets are trapped using acoustic forces in a continuous flow format. Acoustic manipulation is a cell-friendly manipulation technology well-suited for bioparticle trapping.³² Moreover, the method is label-free and operated in a noncontact mode.

In the system, particles (in this case hydrogel droplets) are trapped in an acoustic field generated by a piezoelectric transducer attached to the capillary (Fig. 1). The height of the capillary is equal to a half wavelength of the sound wave; thus, an acoustic standing wave field is generated between the top and bottom of the

capillary [Fig. 1(b)]. This results in a pressure nodal plane at half the height of the capillary and pressure antinodal planes at the top and bottom of the capillary, whereas the velocity field has an anti-nodal plane at half the height of capillary and nodal planes at the top and bottom of the capillary. A particle in an acoustic field will be affected by the primary acoustic radiation force, F^{rad} , given by

$$\mathbf{F}^{\text{rad}} = \frac{4\pi a^3}{3} \nabla \left[f_1 \frac{1}{2} \kappa_{\text{fluid}} \langle p_{\text{in}}^2 \rangle - f_2 \frac{3}{4} \rho_{\text{fluid}} \langle v_{\text{in}}^2 \rangle \right], \quad (1a)$$

$$f_1(\tilde{\kappa}) = 1 - \tilde{\kappa} \quad \text{with} \quad \tilde{\kappa} = \frac{\kappa_{\text{particle}}}{\kappa_{\text{fluid}}}, \quad (1b)$$

$$f_2(\tilde{\rho}) = \frac{2(\tilde{\rho} - 1)}{2\tilde{\rho} + 1} \quad \text{with} \quad \tilde{\rho} = \frac{\rho_{\text{particle}}}{\rho_{\text{fluid}}}, \quad (1c)$$

where a is the radius of the particle, p_{in} is the incoming pressure field, v_{in} is the incoming velocity field, ρ is the density, c is the speed of sound, κ is the compressibility, f_1 is the monopole coefficient, and f_2 is the dipole coefficient.³³ From the equation, it can be seen that a particle that is stiffer and has a higher density than the fluid will be pushed to the pressure nodal plane; thus, particles in water are typically pushed to the midheight of the capillary. Along with the acoustic force in the z-direction, the particles experience a trapping force in the flow direction (x-direction) [Fig. 1(c)]. The transducer is only 1.38 mm in width, and at the edges of the transducer, the acoustic pressure field falls an order of magnitude, resulting in a gradient in the acoustic field in the flow direction.³⁴ At the midheight of the capillary, there is a pressure nodal plane and a velocity antinodal plane. Thus, there is a gradient in the velocity field that generates the trapping forces in the x-direction at this position. In addition, above and below the midheight position, there is a gradient in both the pressure field and the velocity field in the x-direction. The particles used in this article are relatively large and extend out from the midheight plane experiencing these gradients that sums up to the lateral acoustic trapping force.

MATERIALS AND METHODS

An overview of the experimental procedure is shown schematically in Fig. 2. In short, hydrogel droplets are created in a

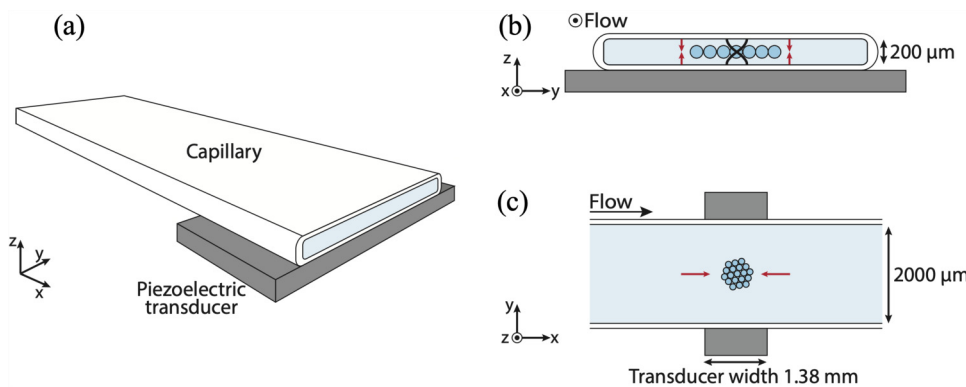


FIG. 1. Trapping device: (a) perspective view, (b) cross-section view, and (c) top view. A localized half wavelength acoustic standing wave field is created in the capillary, causing the hydrogel droplets to be trapped in a well-defined cluster above the transducer. The red arrows indicate the direction of the primary acoustic radiation forces on a hydrogel droplet.

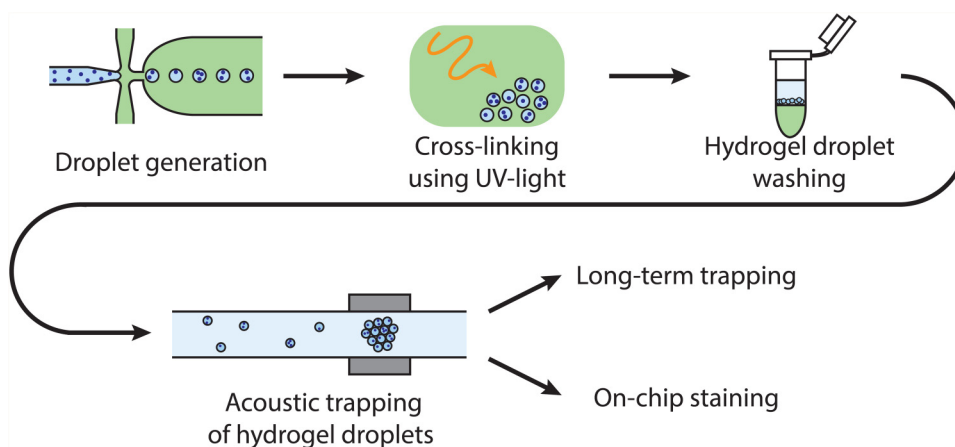


FIG. 2. The experimental procedure.

cross-linkable hydrogel material (hyaluronic acid acrylamide). The hydrogel material is synthesized in-house, and as previously reported in the presence of a photo-initiator and UV-light, a hydrogel network is formed.^{35,36} After cross-linking and droplet washing, the droplets are injected into a second microfluidic system in which acoustic forces are used to trap the droplets. We evaluate the system for two different applications: long-term trapping (3 h) and on-chip staining of the encapsulated cells.

Droplet microfluidic chip fabrication

The droplet microfluidic chips were fabricated in polydimethylsiloxane (PDMS) by soft lithography.³⁷ Briefly, a master mold was created by patterning the structures on a silicon wafer laminated with a 210 μm thick SUEx film (DJ MicroLaminates) using UV-photolithography. A flow focusing design was used for the droplet generation with a 50 μm wide droplet junction. The PDMS (Sylgard 184, Dow Corning) base was mixed with a curing agent at a 10:1 ratio. The PDMS mixture was then degassed and poured over the master, before being cured in the oven for 3 h at 60 °C. PDMS slabs were cut and peeled off the master, and holes for fluid connectors were punched. The channels were sealed by oxygen plasma bonding of the PDMS slabs to glass slides. Finally, the channels were surface-coated with Sigmacote (Sigma-Aldrich) following the protocol from the manufacturer, in order to render the channels hydrophobic.

Hyaluronic acid acrylamide (HA-Am) synthesis

All chemicals used for the synthesis were of chemical grade and obtained from Sigma-Aldrich, unless otherwise reported. Sodium hyaluronate (MW 135 kDa, Lifecore Biomedical) was dissolved in de-ionized water at a concentration of 8 mg/ml. The HCl-H₂N-acrylamide linker (abcr GmbH) was added to the mixture to a final concentration of 0.7 mM, and the mixture was maintained in the dark. Hydroxybenzotriazole (HOBT) was separately dissolved in a 1:1 (v/v) mixture of acetonitrile and de-ionized water at a concentration of 27 mg/ml, and the solution was solubilized by heating. The HOBT solution was then added to the main reaction solution and adjusted to a pH of 6. The coupling reaction was initiated by the addition of N-(3-dimethylaminopropyl)-N'-ethylcarbodiimide

to a final concentration of 1.5 mM. The solution was stirred at room temperature overnight in the dark. The derivative HA was transferred to a dialyzing membrane (MW cutoff 3.5 kDa, SpectrumLabs) against distilled water and 0.24% w/v NaCl for 24 h and adjusted to pH 5. This was filtered to give a clear and transparent solution which was then freeze-dried and stored at -20 °C. The degree of modification of HA-Am was confirmed to be 20% by nuclear magnetic resonance spectroscopy.

Cells

For the encapsulation experiments, a human chondrosarcoma cell line (SW1353) was used. These cells were cultured in high glucose Dulbecco's Modified Eagle Medium (Sigma-Aldrich) with 4500 mg/l glucose, L-glutamine, sodium pyruvate, and sodium bicarbonate and supplemented with 50 mg/l sodium ascorbate, 1% (v/v) penicillin-streptomycin, and 10% (v/v) fetal bovine serum. The cells were incubated at 37 °C with 5% CO₂ and passaged at 80% confluence. Prior to encapsulation, the cells were detached with TrypLE Express (Gibco), fixed in a 3.7% formaldehyde solution and resuspended in phosphate-buffered saline (PBS).

Hyaluronic acid acrylamide hydrogel droplet generation

To prepare the cell-laden HA-Am hydrogel droplets, the fixed cells were resuspended in PBS (4×10^6 cells/ml) with 2% (w/v) HA-Am, 0.4% (w/v) Irgacure 2959 (Sigma-Aldrich) as photo-initiator and 0.5 mM 5-FAM-RGDSC-NH₂ (Innovagen) as fluorescent dye. This solution was then used as the dispersed phase. The droplets used for the confocal microscopy did not contain any cells. Fluorinated oil (HFE-7500, 3M) with 0.5% (v/v) surfactant (Pico-Surf 1, Sphere fluidics) served as the continuous phase. The fluid flows were controlled by syringe pumps (Nemesys, Cetoni) operated in a dispense mode. The flow rate of the dispersed phase was 5 $\mu\text{l}/\text{min}$, and the flow rate of the continuous phase was 300 $\mu\text{l}/\text{min}$. After droplet generation, the droplets were collected off-chip and cross-linked using a long-wave UV-light source (UV LED Curing Lamp, TaoYuan Electron) for 3 s at an intensity of 3.6 W/cm². The cross-linked hydrogel droplets were then

washed twice with surfactant-free oil and resuspended in PBS through centrifugation.

Acoustic trapping device and setup

Figure 3 shows a photograph of the trapping device. The acoustic trapping experiments were performed in a glass capillary (Vitrocom) by actuating a small piezoelectric transducer (0.4 mm thickness, Pz26, Meggitt A/S). The inner cross-section of the capillary is $200\text{ }\mu\text{m} \times 2000\text{ }\mu\text{m}$ (height \times width). A layer of chromium was evaporated on the backside of the capillary to allow for better visualization. Fluid connectors were made by attaching 1 cm long pieces of Tygon-tubing (Saint-Gobain) to the ends of the capillary. The piezoelectric transducer was kerfed to avoid unwanted resonances as described earlier by Hammarström *et al.*,³⁸ and the transducer was soldered onto a printed circuit board (PCB). The transducer was clamped to the capillary in a milled chip holder. To obtain an even clamping pressure, small pads of PDMS were positioned between the capillary and the holder to distribute the pressure. A thin layer of glycerol was added between the capillary and the transducer to achieve good acoustic coupling. An AC-signal from a function generator (33220A, Agilent Technologies) was used to actuate the transducer. The frequency of the applied signal was automatically adjusted by a LabView program developed in-house that continuously scans and finds the optimal resonance frequency.³⁸ In these experiments, the optimal trapping frequency was found to be between 4.0 and 4.1 MHz, and the amplitude of the signal was set to 7 V_{pp} except for the flow rate experiment where the voltage was 10 V_{pp} .

Acoustic trapping experiments

For the acoustic trapping experiments, the hydrogel droplets were withdrawn from an Eppendorf tube and introduced into the capillary using a syringe pump (Nemesys, Cetoni). The maximum flow rate at which a cluster could be held against was determined by first trapping the hydrogel droplets and then reversing and increasing flow rate from $0\text{ }\mu\text{l}/\text{min}$ by step increments of $5\text{ }\mu\text{l}/\text{min}$ until the cluster was pushed out of the trapping zone. An experiment to test long-term trapping of hydrogel droplets was then

performed over 3 h under continuous flow ($10\text{ }\mu\text{l}/\text{min}$). In the final experiment, on-chip staining of the encapsulated cells was performed using Hoechst 33342 nuclei stain (Thermo Scientific). A cluster of hydrogel droplets was trapped and then flushed with Hoechst stain (4 min, $10\text{ }\mu\text{l}/\text{min}$) followed by 10 min of incubation time under stop-flow conditions. The top-view images and videos were acquired using a fluorescence microscope (BX51W1, Olympus) equipped with a camera (XM10, Olympus). The cross-section images were acquired using a confocal system (Fluoview 300, Olympus) using two different laser sources (red and blue). The red laser shows direct reflections from the glass surfaces at the top and bottom of the capillary, while the blue laser is used to excite green fluorescence. To allow for imaging of the hydrogel droplets an aqueous solution of fluorescein was injected into the trapping capillary causing the entire capillary volume except the hydrogel droplets to fluoresce strongly in green when excited by the blue laser. Thus, the droplets appear as dark shadows in the green fluorescent fluid as it takes time before the fluorescein solution diffuses into the hydrogel droplets.

RESULTS AND DISCUSSION

Hydrogel droplet generation

Cell-laden hydrogel droplets were generated and cross-linked off-chip using UV-light and transferred to PBS. The cross-linked hydrogel droplets were observed to swell after they were washed and transferred from fluorinated oil to PBS. For these specific flow settings and channel dimensions, the average diameter of the hydrogel droplets after swelling was $107 \pm 9\text{ }\mu\text{m}$ (s.d., $n = 36$). The average number of cells per droplet was determined by manual counting to be 9.4 ± 3.2 cells/droplet (s.d., $n = 203$).

Hydrogel droplet trapping

The hydrogel droplets were withdrawn from an Eppendorf tube into the trapping capillary. Without the application of the ultrasound the hydrogel droplets simply flowed through the capillary, but when the ultrasound was applied, the hydrogel droplets were trapped in the lateral direction (x-direction) into a cluster above the transducer. In Fig. 4, an image sequence of acoustic trapping over time is shown. The full video of the trapping is available in the [supplementary material](#) (ESI 1). One advantage of the presented trapping technology is that the trapped cluster can be released on-demand by simply turning off the ultrasound (time point 30 s).

The hydrogel droplets were also positioned in the vertical direction (z-direction) due to the standing wave field between the top and bottom of the capillary. The vertical position of the trapped cluster was studied using confocal microscopy. As shown in Fig. 5, the droplets were arranged into a monolayer at the mid-height of the capillary. This proves experimentally that the hydrogel droplets have a positive acoustic contrast factor, as the droplets are pushed to the pressure nodal plane. The monolayer formation allows the fluid to pass both above and below the droplet cluster, ensuring proper media exchange for all droplets. The formation of a monolayer is also advantageous for optical monitoring using standard microscope configurations.

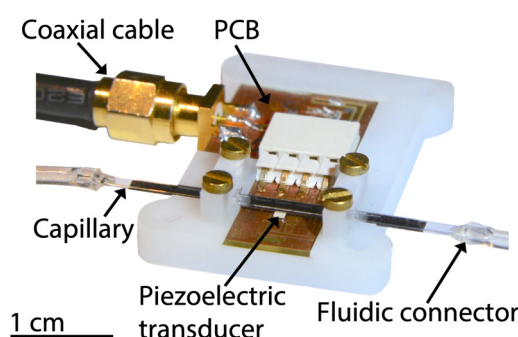


FIG. 3. The acoustic trapping device.

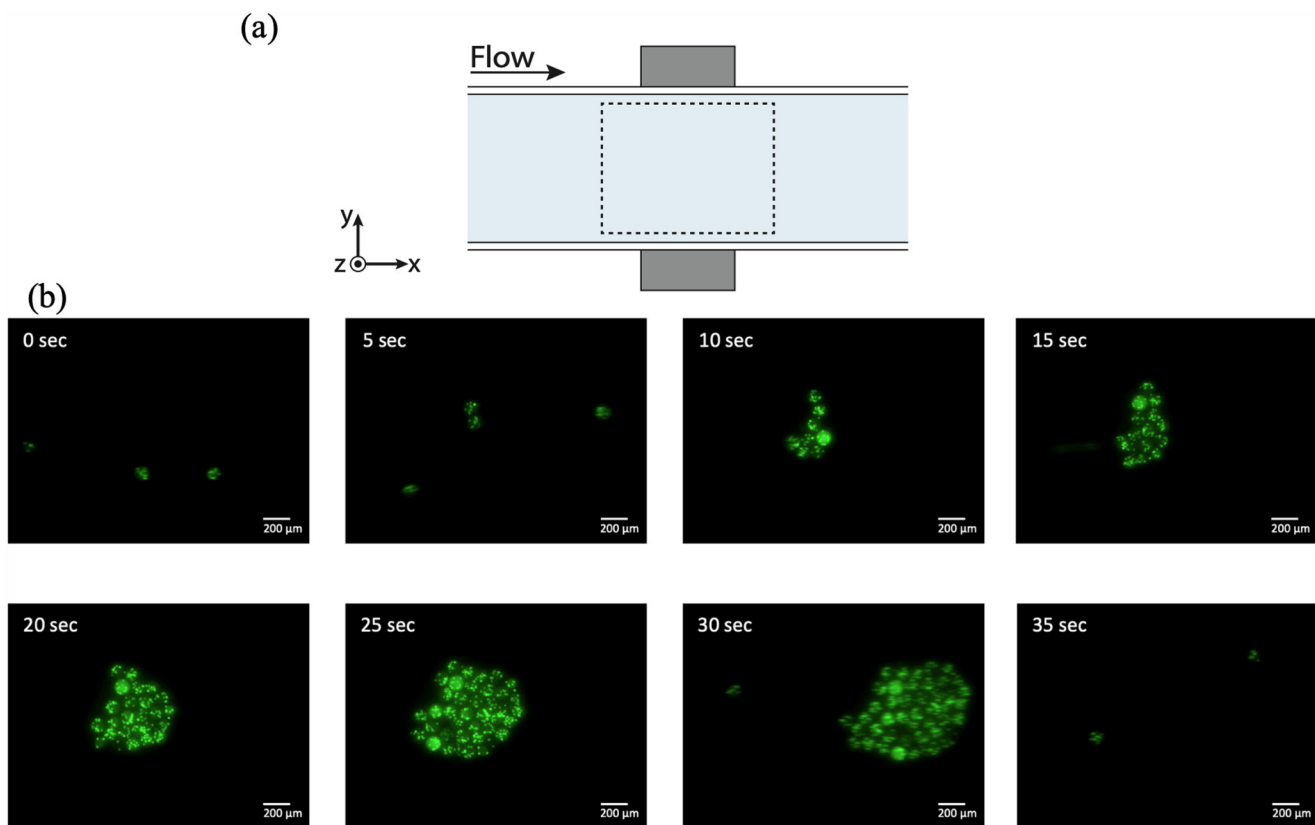


FIG. 4. (a) Approximate field of view of the photographs in (b). (b) Without acoustic trapping (time point 0 s), the hydrogel droplets flow through the capillary and pass the trapping site. At actuation of the transducer (time point 5–25 s), a standing wave field is created in the capillary causing the hydrogel droplets to be trapped in a cluster. When the ultrasound is turned off again the cluster is released and flow downstream (time point 30–35 s). The images are top views, and the direction of flow is toward the right in the images. The bright spots within the droplets are individual cells.

Flow rate experiment

The flow rate at which the drag force exceeded the acoustic trapping force was investigated for hydrogel droplet clusters containing between 32 and 50 hydrogel droplets. The maximum flow rate the cluster could be held against was determined to be $76 \pm 12 \mu\text{l}/\text{min}$ (s.d., $n = 5$), which corresponds to an average flow speed of 3.2 mm/s. This value of the maximum flow velocity is in the same order of

magnitude of what has been reported for bead trapping in similar systems.²⁷ In all five replicates, the entire cluster was lost at once. A flow rate of a few tens of $\mu\text{l}/\text{min}$ is sufficient for perfusion in most applications as that corresponds to a fluid exchange in the capillary and the external tubings (in total approximately $40 \mu\text{l}$) in only a couple of minutes. It is, therefore, highly unlikely that flow rates exceeding $70 \mu\text{l}/\text{min}$ would be needed.

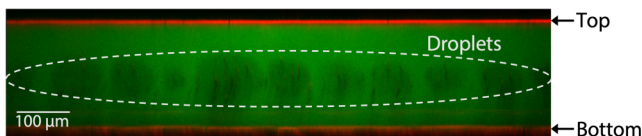


FIG. 5. Confocal image showing the cross-section of the capillary. With ultrasound on, the droplets are positioned at the midheight of the capillary. The red lines are reflections from the top and bottom of the capillary, and the green fluorescence comes from the aqueous solution of fluorescein used only in this experiment.

Long-term hydrogel droplet trapping

One application of droplet trapping is monitoring of the encapsulated cells over time. To demonstrate this, a cluster of hydrogel droplets were trapped for 3 h and continuously perfused with PBS at $10 \mu\text{l}/\text{min}$ (Fig. 6). As seen from the snapshots taken at the start and end of the experiment, the system was stable and no hydrogel droplets were lost during the experiment.

Moreover, as seen from Fig. 6, the position of the trapped hydrogel droplets in the cluster was stationary in the capillary over time. This is advantageous in many applications as it simplifies automatic image analysis of the encapsulated cells within the droplets.

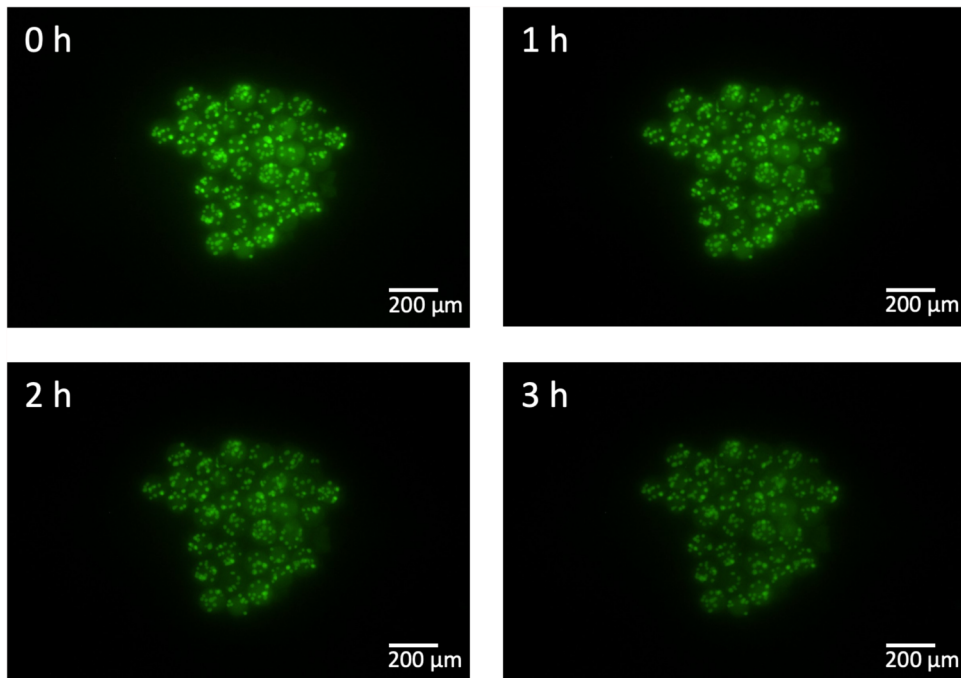


FIG. 6. Long-term trapping of hydrogel droplets for 3 h. The difference in fluorescence intensity is due to bleaching. The images are top-view images, and the bright spots within the droplets are individual cells.

On-chip cell nuclei staining

In order to explore another application of the trapping system, an on-chip staining procedure (Hoechst staining) of the encapsulated cells was performed. Cell-laden hydrogel droplets were introduced into the capillary and trapped in a cluster [Fig. 7(a)]. Prior to Hoechst staining, the cells were not visible in the DAPI channel (blue), but the droplets and the cells were visible in the FITC channel (green) due to the addition of a green fluorescent dye (5-FAM-RGDSC-NH₂) before the

droplet generation. In the experiment, the trapped hydrogel droplets were perfused with Hoechst stain and then incubated under stop-flow conditions for 10 min. After staining, the cells were clearly visible also in the DAPI channel [Fig. 7(b)]. As the Hoechst stain only fluoresces when bound to double-stranded DNA, no wash step was needed before visualization. This experiment shows that the presented droplet trapping technology is well-suited for on-chip biological assays such as cell nuclei staining.

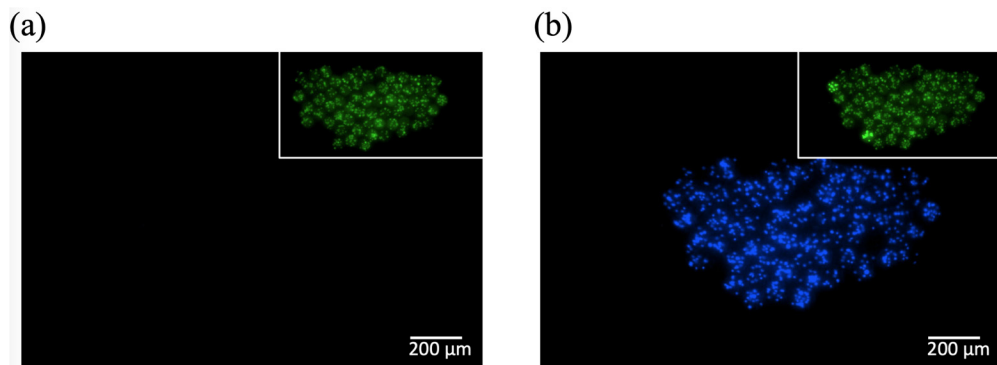


FIG. 7. Acoustic trapping followed by Hoechst staining on-chip. (a) Hydrogel droplets are trapped, but before Hoechst staining the cells are not visible in the DAPI channel (blue). (b) After Hoechst staining the cells are visible in the DAPI channel. The insets show photographs taken under the same field of view in the FITC channel (green) to demonstrate the presence of trapped hydrogel droplets in both (a) and (b). The images are top-view images, and the bright spots within the droplets are individual cells.

CONCLUSION

In this work, we demonstrate a microfluidic system for non-contact trapping of cell-laden hydrogel droplets in a microfluidic channel using acoustic forces. The presented method has several advantages, such as being label-free, compatible with *in situ* optical microscopy, and offering the possibility to release the hydrogel droplets on-demand. Moreover, as the droplet cluster forms a monolayer and is positioned at the midheight of the capillary, fluid can pass both over and under the cluster that facilitates proper media exchange for all droplets. Two examples of future applications of this platform include long-term trapping and on-chip staining of encapsulated cells, as demonstrated in our work. We believe that the presented acoustic trapping system is versatile and has potential to be integrated in various types of droplet-based assays where different reagents or fresh cell media need to be added to the cell-laden hydrogel droplets.

SUPPLEMENTARY MATERIAL

In the [supplementary material](#), a video showing trapping of hydrogel droplets is available.

ACKNOWLEDGMENTS

This work was funded by the Swedish Research Council, the Crafoord Foundation, Foundation Olle Engkvist Byggmästare, Swedish Foundation for Strategic Research, and the Royal Physiographic Society of Lund. The authors would also like to thank Maria Antfolk (Lund University) for providing material for the initial acoustic trapping studies, Mikael Evander (Lund University) for help with the fabrication of the trapping device, Gry Hulsart Billström (Uppsala University) for the kind gift of SW1353 cells, and Dmitri A. Ossipov and Liyang Shi (Uppsala University) for advice on the synthesis of the hydrogel material.

REFERENCES

- ¹I. S. Casadevall and A. DeMello, *Chem. Commun.* **47**, 1936 (2011).
- ²S. Mashaghi, A. Abbaspourrad, D. A. Weitz, and A. M. van Oijen, *Trends Anal. Chem.* **82**, 118 (2016).
- ³L. Shang, Y. Cheng, and Y. Zhao, *Chem. Rev.* **117**, 7964 (2017).
- ⁴T. Schneider, J. Kreutz, and D. T. Chiu, *Anal. Chem.* **85**, 3476 (2013).
- ⁵M. Tenje, A. Fornell, M. Ohlin, and J. Nilsson, *Anal. Chem.* **90**, 1434 (2018).
- ⁶M. T. Guo, A. Rotem, J. A. Heyman, and D. A. Weitz, *Lab Chip* **12**, 2146 (2012).
- ⁷N. Shembekar, C. Chaipan, R. Utharala, and C. A. Merten, *Lab Chip* **16**, 1314 (2016).
- ⁸C. Martino and A. J. DeMello, *Interface Focus* **6**, 20160011 (2016).
- ⁹W. Jiang, M. Li, Z. Chen, and K. W. Leong, *Lab Chip* **16**, 4482 (2016).
- ¹⁰C. Frantz, K. M. Stewart, and V. M. Weaver, *J. Cell Sci.* **123**, 4195 (2010).
- ¹¹D. Velasco, E. Tumarkin, and E. Kumacheva, *Small* **8**, 1633 (2012).
- ¹²T. Rossow, P. S. Lienemann, and D. J. Mooney, *Macromol. Chem. Phys.* **218**, 1600380 (2017).
- ¹³H. Huang, Y. Yu, Y. Hu, X. He, O. Berk Usta, and M. L. Yarmush, *Lab Chip* **17**, 1913 (2017).
- ¹⁴F. Ullah, M. B. H. Othman, F. Javed, Z. Ahmad, and H. M. Akil, *Mater. Sci. Eng. C* **57**, 414 (2015).
- ¹⁵T. Rossow, J. A. Heyman, A. J. Ehrlicher, A. Langhoff, D. A. Weitz, R. Haag, and S. Seiffert, *J. Am. Chem. Soc.* **134**, 4983 (2012).
- ¹⁶W. H. Tan and S. Takeuchi, *Adv. Mater.* **19**, 2696 (2007).
- ¹⁷Y. Ma, M. P. Neubauer, J. Thiele, A. Fery, and W. T. S. Huck, *Biomater. Sci.* **2**, 1661 (2014).
- ¹⁸C. H. Choi, H. Wang, H. Lee, J. H. Kim, L. Zhang, A. Mao, D. J. Mooney, and D. A. Weitz, *Lab Chip* **16**, 1549 (2016).
- ¹⁹D. J. Collins, A. Neild, A. deMello, A.-Q. Liu, and Y. Ai, *Lab Chip*, **15** 3439 (2015).
- ²⁰Z. Zhu and C. J. Yang, *Acc. Chem. Res.* **50**, 22 (2017).
- ²¹A. Huebner, D. Bratton, G. Whyte, M. Yang, A. J. DeMello, C. Abell, and F. Hollfelder, *Lab Chip* **9**, 692 (2009).
- ²²J. H. Jung, G. Destgeer, J. Park, H. Ahmed, K. Park, and H. J. Sung, *Anal. Chem.* **89**, 2211 (2017).
- ²³R. W. Rambach, K. Linder, M. Heymann, and T. Franke, *Lab Chip* **17**, 3422 (2017).
- ²⁴S. Sart, R. F. X. Tomasi, G. Amselem, and C. N. Baroud, *Nat. Commun.* **8**, 469 (2017).
- ²⁵J. A. Burdick and G. D. Prestwich, *Adv. Mater.* **23**, H41 (2011).
- ²⁶M. N. Collins and C. Birkinshaw, *Carbohydr. Polym.* **92**, 1262 (2013).
- ²⁷B. Hammarström, M. Evander, H. Barbeau, M. Bruzelius, J. Larsson, T. Laurell, and J. Nilsson, *Lab Chip* **10**, 2251 (2010).
- ²⁸M. Evander, O. Gidlöf, B. Olde, D. Erlinge, and T. Laurell, *Lab Chip* **15**, 2588 (2015).
- ²⁹D. J. Collins, B. Morahan, J. Garcia-Bustos, C. Doerig, M. Plebanski, and A. Neild, *Nat. Commun.* **6**, 8686 (2015).
- ³⁰F. Guo, Z. Mao, Y. Chen, Z. Xie, J. P. Lata, P. Li, L. Ren, J. Liu, J. Yang, M. Dao, S. Suresh, and T. J. Huang, *Proc. Natl. Acad. Sci. U.S.A.* **113**, 1522 (2016).
- ³¹M. Tenje, H. Xia, M. Evander, B. Hammarström, A. Tojo, S. Belák, T. Laurell, and N. LeBlanc, *Anal. Chim. Acta* **853**, 682 (2015).
- ³²M. Wiklund, *Lab Chip* **12**, 2018 (2012).
- ³³H. Bruus, *Lab Chip* **12**, 1014 (2012).
- ³⁴M. W. H. Ley and H. Bruus, *Phys. Rev. Appl.* **8**, 024020 (2017).
- ³⁵L. Shi, H. Carstensen, K. Höglz, M. Lunzer, H. Li, J. Hilborn, A. Ovsianikov, and D. A. Ossipov, *Chem. Mater.* **29**, 5816 (2017).
- ³⁶L. Shi, F. Wang, W. Zhu, Z. Xu, S. Fuchs, J. Hilborn, L. Zhu, Q. Ma, Y. Wang, X. Weng, and D. A. Ossipov, *Adv. Funct. Mater.* **27**(37), 1 (2017).
- ³⁷D. C. Duffy, J. C. McDonald, O. J. A. Schueller, and G. M. Whitesides, *Anal. Chem.* **70**, 4974 (1998).
- ³⁸B. Hammarström, M. Evander, J. Wahlström, and J. Nilsson, *Lab Chip* **14**, 1005 (2014).